Signals of new heavy scalars in the flavor-aligned 2HDM

Howard E. Haber

June 5, 2023

Outline

1. Experimental hints for new heavy scalars
   - Scenario 1: m_A=610 GeV and m_H=290 GeV, with A → ZH, H → bb
   - Scenario 2: m_A=400 GeV, with A → t t and A → τ+τ-

2. Basis-independent treatment of the Aligned two Higgs doublet model
   - Quick review of the general 2HDM in the Higgs basis
   - Defining the Aligned 2HDM (A2HDM)
   - Types I, II, X and Y Yukawa interactions as special cases of the A2HDM
   - CP-conserving A2HDM

3. Accommodating hints for heavy scalars in the A2HDM
   - Signals that are not compatible with Types I, II, X, and Y Yukawa couplings

This work is based on: J.M. Connell, P. Ferreira, and H. E. Haber, arXiv: 2302.13697

Experimental hints for new heavy scalars

	m_H	m_A	A2HDM interpretation of the excess of events
Scenario 1	290 GeV	610 GeV	$gg \to A \to ZH$, where $H \to b\bar{b}$ and $Z \to \ell^+\ell^-$ [18]
Scenario 2	> 450 GeV	400 GeV	$gg \to A \to \tau^+\tau^-$ [20] $gg \to b\bar{b}A$, where $A \to \tau^+\tau^-$ [20] $gg \to A \to t\bar{t}$ [21]

Table 4: Scenario 1 is based on an ATLAS excess of events with a local (global) significance of $3.1(1.3)\sigma$, where the observed lepton is $\ell = e, \mu$. Scenario 2 is based on an ATLAS excess of $\tau^+\tau^-$ events with an invariant mass of around 400 GeV, with local significances of 2.7σ in the gg fusion production channel and 2.2σ in the b-associated production channel. The CMS Collaboration sees no excess, but still leaves some room for a possible signal. The ATLAS data does not distinguish between H and A production. However, the CMS excess of $t\bar{t}$ events with an invariant mass of around 400 GeV, with a local (global) significance of $3.5(1.9)\sigma$, favors identifying the excess at 400 GeV with A production.

[18] G. Aad et al. [ATLAS Collaboration], Eur. Phys. J. C **81**, 396 (2021) [arXiv:2011.05639 [hep-ex]].

[19] G. Aad et al. [ATLAS Collaboration], Phys. Rev. Lett. **125**, 051801 (2020) [arXiv:2002.12223 [hep-ex]].

[20] See Fig. 08 in https://atlas.web.cern.ch/Atlas/GROUPS/PHYSICS/PAPERS/HDBS-2018-46/, which appeared in auxiliary material that was not included in Ref. [19].

[21] A.M. Sirunyan et al. [CMS Collaboration], JHEP **04**, 171 (2020) [arXiv:1908.01115 [hep-ex]].

Scenario 1: m_A = 610 GeV and m_H = 290 GeV, with pp $\rightarrow$ A $\rightarrow$ ZH, followed by H $\rightarrow$ bb and Z $\rightarrow$ lepton pairs

Left-hand plots: expected upper limits

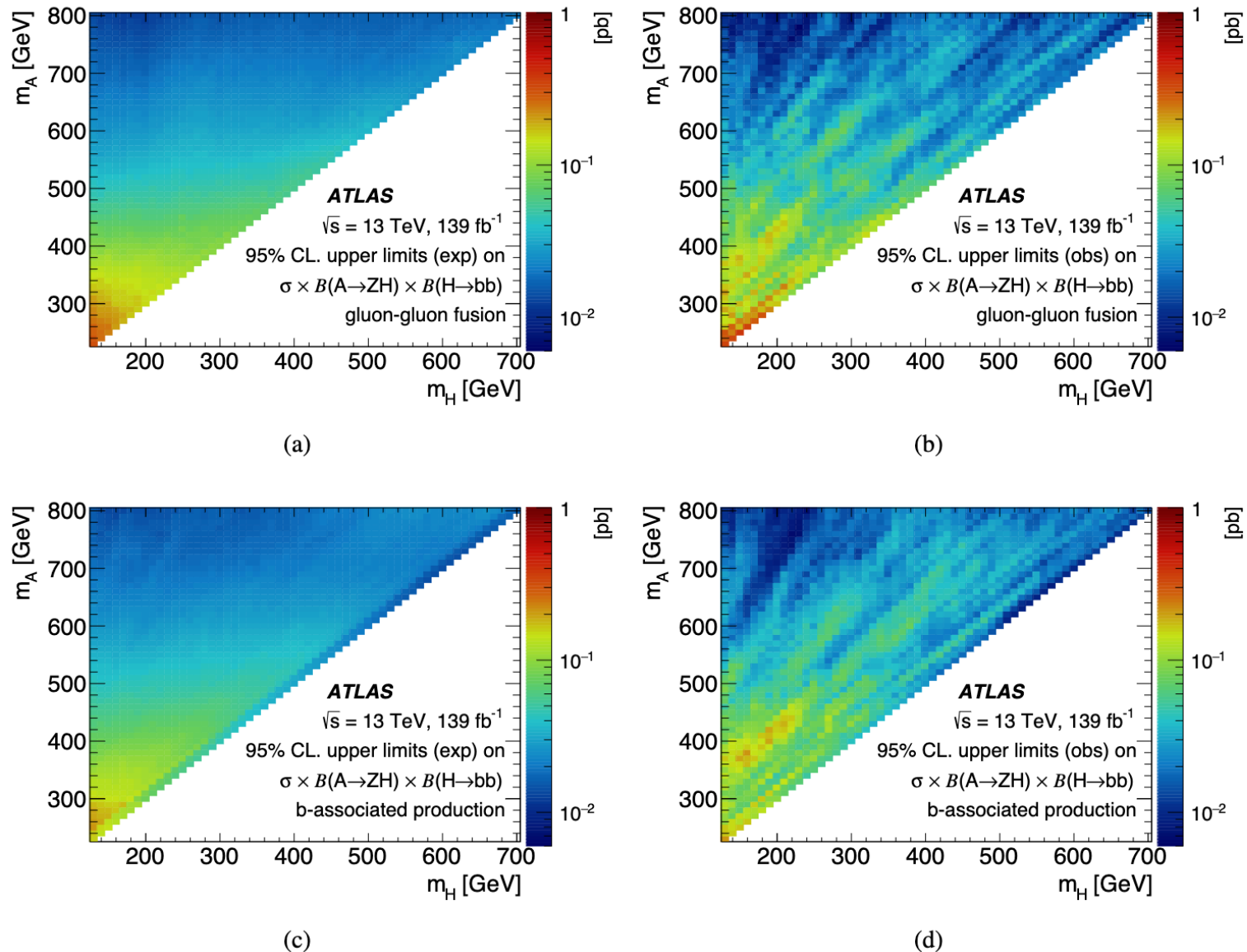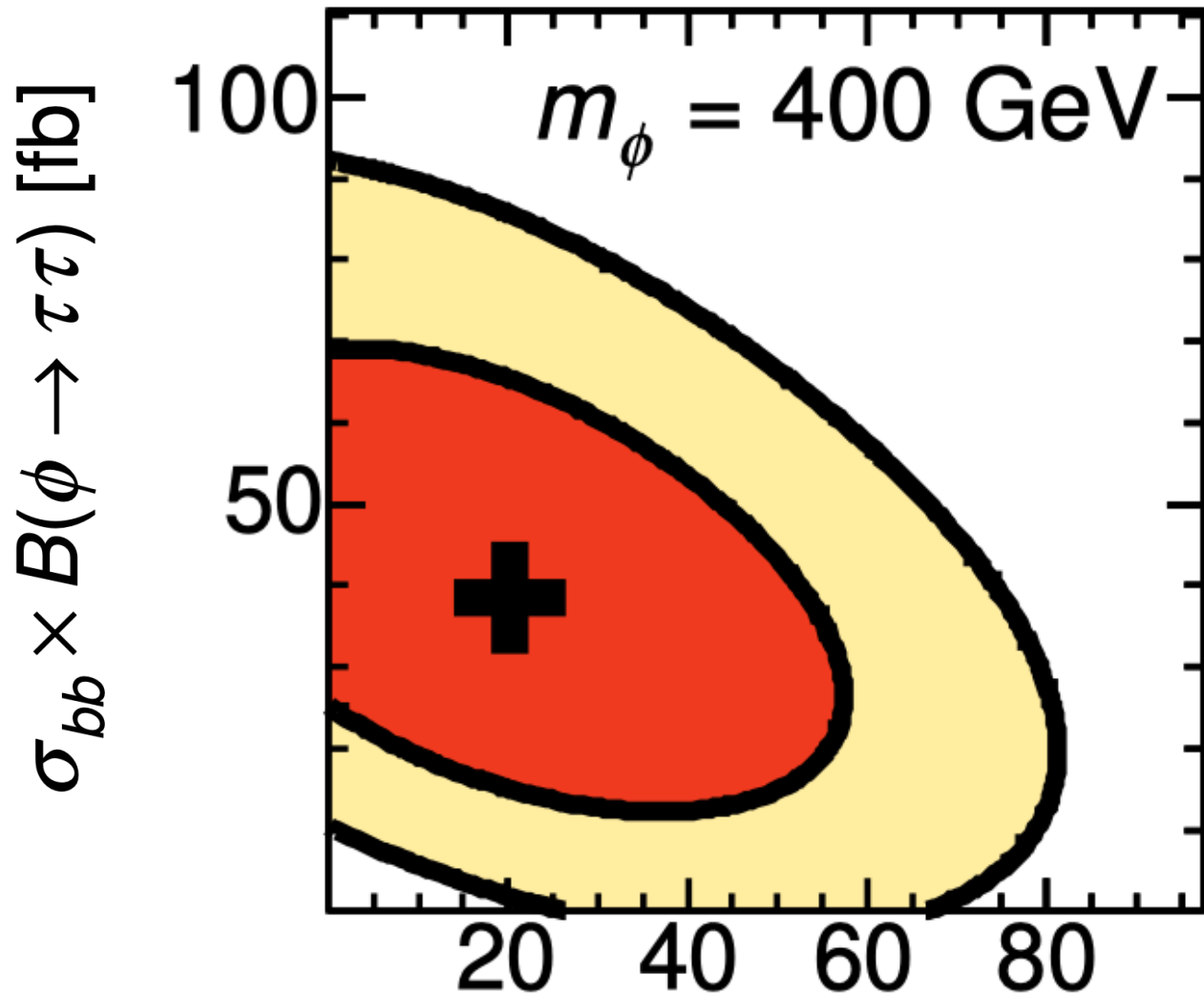Right-hand plots: Observed upper limits (suggesting an excess of events)

Figure 9: Upper bounds at 95% CL on the production cross section times the branching ratio $B(A \rightarrow ZH) \times B(H \rightarrow bb)$ in pb for (a, b) gluon–gluon fusion and (c, d) b-associated production. The expected upper limits are shown in (a) and (c) and the observed upper limits are shown in (b) and (d).

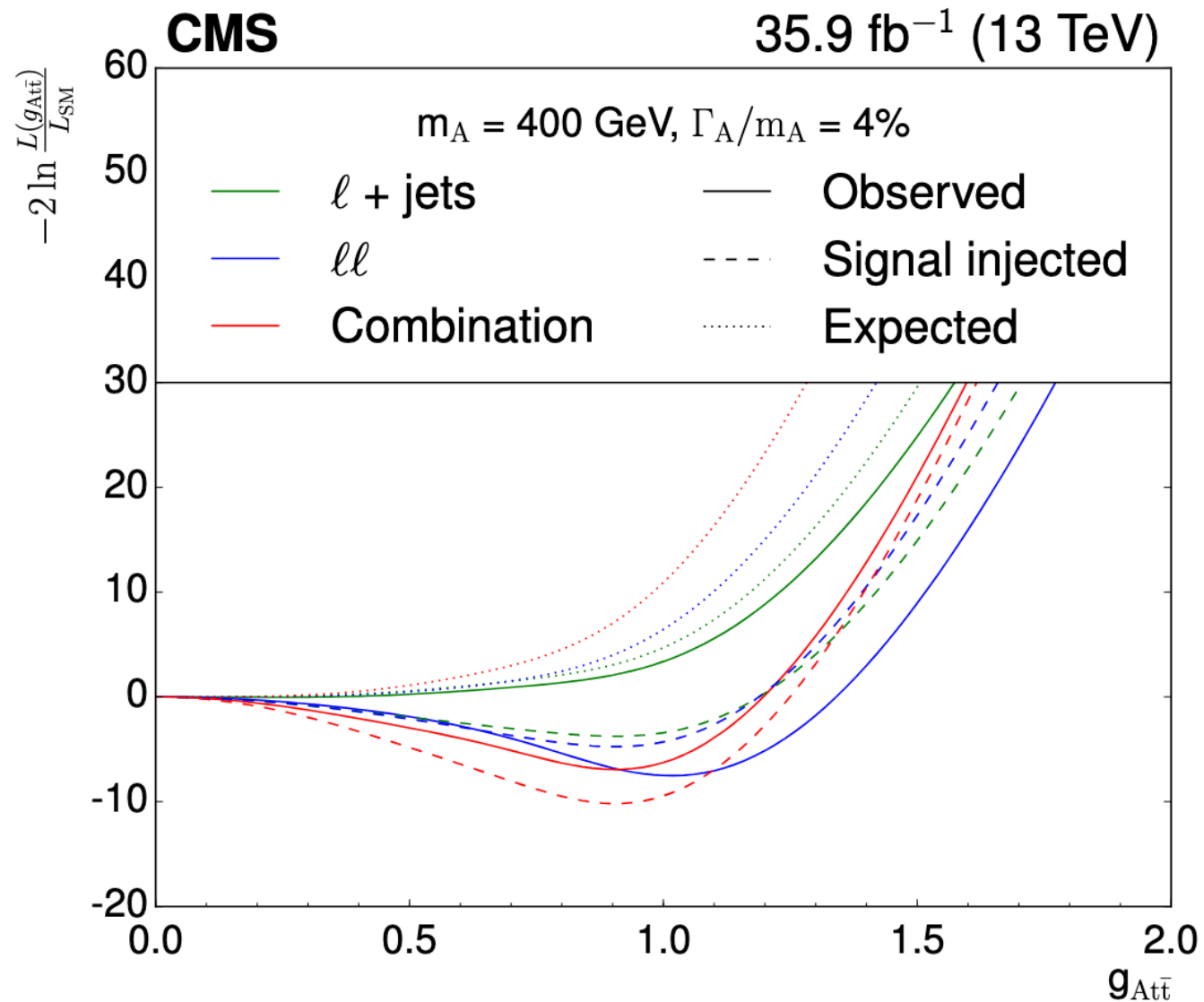Scenario 2: m_A = 400 GeV, with pp → A → $\tau^+\tau^-$

Figure 7. Scans of profiled likelihood for the pseudoscalar hypothesis with $m_A = 400\,\text{GeV}$ and $\Gamma_A/m_A = 4\%$. The scans are shown for the single- and dilepton channels separately, as well as for the combination.

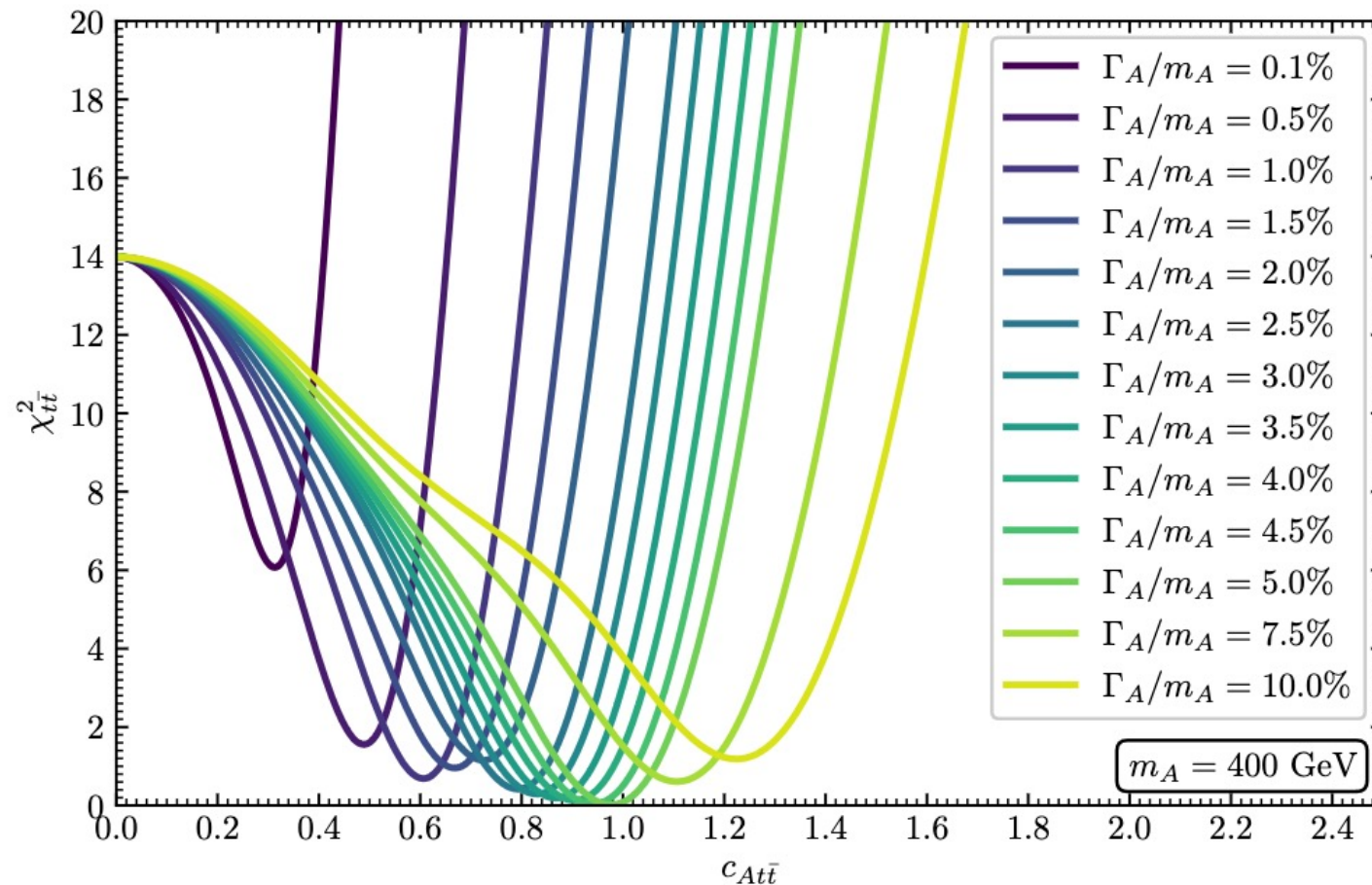Figure 1: $\chi^2_{t\bar{t}}$ as a function of $c_{At\bar{t}}$ assuming $m_A = 400$ GeV for the different width hypotheses used in the experimental analysis [6, 31]. $\chi^2_{t\bar{t}}$ is defined relative to the best fit point.

Figure taken from: T. Biekötter, A. Grohsjean, S. Heinemeyer, C. Schwanenberger, and G. Weiglein, Eur. J. Phys. C 82, 483 (2022)

The 2HDM consists of two $Y = 1$ scalar doublet fields Φ_1 and Φ_2. The kinetic energy terms are invariant under $\Phi_i \rightarrow U_{ij}\Phi_j$ ($i, j \in \{1, 2\}$ with an implicit sum over j), where U is a 2×2 unitary matrix, which constitutes a change of scalar field basis.

If no additional symmetries are present, the choice of basis is arbitrary. Only basis-invariant quantities are physical. This motivates the introduction of the Higgs basis $\{\mathcal{H}_1, \mathcal{H}_2\}$ where $\langle \mathcal{H}_1^0 \rangle = v/\sqrt{2}$ and $\langle \mathcal{H}_2^0 \rangle = 0$, where $v \simeq 246$ GeV.

The Higgs basis is unique up to a phase rotation of $\mathcal{H}_2$.

In the Higgs basis, the scalar potential is:

$$\mathcal{V} = Y_1 \mathcal{H}_1^\dagger \mathcal{H}_1 + Y_2 \mathcal{H}_2^\dagger \mathcal{H}_2 + [Y_3 e^{-i\eta} \mathcal{H}_1^\dagger \mathcal{H}_2 + \text{h.c.}] +$$

$$\tfrac{1}{2} Z_1 (\mathcal{H}_1^\dagger \mathcal{H}_1)^2 + \tfrac{1}{2} Z_2 (\mathcal{H}_2^\dagger \mathcal{H}_2)^2 + Z_3 (\mathcal{H}_1^\dagger \mathcal{H}_1)(\mathcal{H}_2^\dagger \mathcal{H}_2) + Z_4 (\mathcal{H}_1^\dagger \mathcal{H}_2)(\mathcal{H}_2^\dagger \mathcal{H}_1)$$

$$+ \left\{ \tfrac{1}{2} Z_5 e^{-2i\eta} (\mathcal{H}_1^\dagger \mathcal{H}_2)^2 + \left[Z_6 e^{-i\eta} (\mathcal{H}_1^\dagger \mathcal{H}_1) + Z_7 e^{-i\eta} (\mathcal{H}_2^\dagger \mathcal{H}_2) \right] \mathcal{H}_1^\dagger \mathcal{H}_2 + \text{h.c.} \right\} .$$

The phase $e^{-i\eta}$ reflects the nonuniqueness of the Higgs basis. Under a change of basis, $\Phi_i \to U_{ij} \Phi_j$, the parameters Y_1, Y_2 and $Z_1, \ldots Z_4$ are invariant whereas

$$[Y_3, Z_6, Z_7, e^{i\eta}] \to (\det\ U)^{-1}[Y_3, Z_6, Z_7, e^{i\eta}]\,,$$

$$Z_5 \to (\det\ U)^{-2} Z_5\,.$$

The minimization of the scalar potential in the Higgs basis yields

$$Y_1 = -\tfrac{1}{2} Z_1 v^2\,, \qquad Y_3 = -\tfrac{1}{2} Z_6 v^2\,.$$

The 3×3 neutral scalar squared mass matrix is:

$$\mathcal{M}^2 = v^2 \begin{pmatrix} Z_1 & \mathrm{Re}(Z_6 e^{-i\eta}) & -\mathrm{Im}(Z_6 e^{-i\eta}) \\ \mathrm{Re}(Z_6 e^{-i\eta}) & \frac{1}{2}\left[Z_{34} + \mathrm{Re}(Z_5 e^{-2i\eta})\right] + Y_2/v^2 & -\frac{1}{2}\mathrm{Im}(Z_5 e^{-2i\eta}) \\ -\mathrm{Im}(Z_6 e^{-i\eta}) & -\frac{1}{2}\mathrm{Im}(Z_5 e^{-2i\eta}) & \frac{1}{2}\left[Z_{34} - \mathrm{Re}(Z_5 e^{-2i\eta})\right] + Y_2/v^2 \end{pmatrix}$$

with respect to the $\{\sqrt{2}\,\mathrm{Re}\,\mathcal{H}_1^0 - v,\ \sqrt{2}\,\mathrm{Re}\,\mathcal{H}_2^0,\ \sqrt{2}\,\mathrm{Im}\,\mathcal{H}_2^0\}$ basis, where $Z_{34} \equiv Z_3 + Z_4$.

Diagonalize $\mathcal{M}^2$ to obtain the scalar masses,

$$R\mathcal{M}^2 R^\mathsf{T} = \mathrm{diag}\left(m_1^2,\, m_2^2,\, m_3^2\right),$$

where $R \equiv R_{12}R_{13}R_{23}$ is the product of three rotation matrices parametrized by three basis-invariant angles, θ_{12}, θ_{13} and θ_{23}, respectively.

Denoting the neutral scalar mass eigenstates by h_k $(k = 1, 2, 3)$,

$$\mathcal{H}_1 = \begin{pmatrix} G^+ \\ \dfrac{1}{\sqrt{2}} \left(v + iG + \sum_{k=1}^{3} q_{k1} h_k \right) \end{pmatrix}, \qquad e^{i\theta_{23}} \mathcal{H}_2 = \begin{pmatrix} H^+ \\ \dfrac{1}{\sqrt{2}} \sum_{k=1}^{3} q_{k2} h_k \end{pmatrix}.$$

where the basis-invariant quantities $q_{k\ell}$ depend on θ_{12} and θ_{13} as indicated in the table below, where $c_{ij} \equiv \cos\theta_{ij}$ and $s_{ij} \equiv \sin\theta_{ij}$.

k	q_{k1}	q_{k2}
1	$c_{12}c_{13}$	$-s_{12} - ic_{12}s_{13}$
2	$s_{12}c_{13}$	$c_{12} - is_{12}s_{13}$
3	s_{13}	ic_{13}

Without loss of generality, one can set $\theta_{23} = 0$.

Higgs-fermion Yukawa couplings

After determining the quark mass eigenstate fields and the scalar mass eigenstate fields, the resulting 2HDM Yukawa couplings are

$$-\mathscr{L}_Y = \overline{U}\left\{\frac{\boldsymbol{M_U}}{v}q_{k1} + \frac{1}{\sqrt{2}}\left[q_{k2}^* \,\boldsymbol{\rho^U} P_R + q_{k2}\,\boldsymbol{\rho^{U\dagger}} P_L\right]\right\}U h_k$$

$$+\overline{D}\left\{\frac{\boldsymbol{M_D}}{v}q_{k1} + \frac{1}{\sqrt{2}}\left[q_{k2}\,\boldsymbol{\rho^{D\dagger}} P_R + q_{k2}^*\,\boldsymbol{\rho^D} P_L\right]\right\}D h_k$$

$$+\overline{E}\left\{\frac{\boldsymbol{M_E}}{v}q_{k1} + \frac{1}{\sqrt{2}}\left[q_{k2}\,\boldsymbol{\rho^{E\dagger}} P_R + q_{k2}^*\,\boldsymbol{\rho^E} P_L\right]\right\}E h_k$$

$$+\left\{\overline{U}\left[\boldsymbol{K}\boldsymbol{\rho^{D\dagger}} P_R - \boldsymbol{\rho^{U\dagger}}\boldsymbol{K} P_L\right]D H^+ + \overline{N}\boldsymbol{\rho^{E\dagger}} P_R E H^+ + \text{h.c.}\right\},$$

summed over $k \in \{1, 2, 3\}$, where $P_{R,L} \equiv \frac{1}{2}(1\pm\gamma_5)$, $\boldsymbol{K}$ is the CKM matrix, and the mass-eigenstate quark and lepton fields are $D = (d, s, b)^\mathsf{T}$, $U \equiv (u, c, t)^\mathsf{T}$, $E = (e, \mu, \tau)^\mathsf{T}$, and $N = (\nu_e, \nu_\mu, \nu_\tau)^\mathsf{T}$, with corresponding diagonal mass matrices $\boldsymbol{M_F}$ and complex invariant Yukawa matrices $\boldsymbol{\rho^F}$ ($F = U, D, E$),

The Aligned 2HDM (A2HDM)

The A2HDM posits that the Yukawa matrices $\boldsymbol{\rho}^{\boldsymbol{F}}$ are proportional to the corresponding fermion mass matrix $\boldsymbol{M_F}$.[*] We define the basis-invariant *flavor-alignment parameters* a^F via,

$$\boldsymbol{\rho}^{\boldsymbol{F}} = \frac{\sqrt{2}a^F\boldsymbol{M_F}}{v}, \qquad \text{for } F = U, D, E.$$

The resulting Yukawa couplings are:

$$-\mathscr{L}_Y = \frac{1}{v}\overline{U}\boldsymbol{M_U}\sum_{k=1}^{3}\left\{q_{k1} + q_{k2}^* a^U P_R + q_{k2}a^{U*}P_L\right\}Uh_k$$

$$+\frac{1}{v}\sum_{F=D,E}\left\{\overline{F}\boldsymbol{M_F}\sum_{k=1}^{3}(q_{k1} + q_{k2}a^{F*}P_R + q_{k2}^* a^F P_L)\,Fh_k\right\}$$

$$+\frac{\sqrt{2}}{v}\left\{\overline{U}\left[a^{D*}\boldsymbol{KM_D}P_R - a^{U*}\boldsymbol{M_UK}P_L\right]DH^+ + a^{E*}\overline{N}\boldsymbol{M_E}P_R EH^+ + \text{h.c.}\right\}.$$

[*]A. Pich and P. Tuzon, Phys. Rev. D 80, 091702 (2009).

Special cases of the A2HDM

The A2HDM as formulated above is not radiatively stable. There are three possible approaches.

- Treat the A2HDM phenomenologically and let experiment decide the structure of the Yukawa sector.

- Impose the A2HDM conditions at a UV scale and then use RG evolution to generate FCNCs mediated by neutral scalars at the EW scale which may be consistent with low energy data.

- Impose a symmetry of the Higgs Lagrangian (which may be softly broken) to naturally eliminate tree-level FCNCs mediated by neutral scalars.

Types I, II, X and Y Yukawa Lagrangians

Impose a $\mathbb{Z}_2$ symmetry on the dimension-four terms of the Higgs Lagrangian. This defines the Φ-basis, where the terms

$$\mathcal{V} \supset (\lambda_6 \Phi_1^\dagger \Phi_1 + \lambda_7 \Phi_2^\dagger \Phi_2) \Phi_1^\dagger \Phi_2 + \text{h.c.}$$

are absent after imposing the discrete symmetry $\Phi_1 \to +\Phi_1$, $\Phi_2 \to -\Phi_2$. In the Φ-basis,

$$\langle \Phi_1^0 \rangle = v \cos \beta / \sqrt{2} \,, \qquad \langle \Phi_2^0 \rangle = e^{i\xi} v \sin \beta / \sqrt{2} \,,$$

which defines the angle β and the phase angle ξ. Due to the $\mathbb{Z}_2$ symmetry, these parameters are now physical.

There exists a scalar field basis where $\lambda_6 = \lambda_7 = 0$ if and only if the following two conditions are satisfied:[†]

$$(Z_1 - Z_2)\big[Z_{34}|Z_{67}|^2 - Z_2|Z_6|^2 - Z_1|Z_7|^2 - Z_{12}\operatorname{Re}(Z_6^* Z_7)\big]$$
$$+ \operatorname{Re}(Z_5^* Z_{67}^2) - 2|Z_{67}|^2\big(|Z_6|^2 - |Z_7|^2\big) = 0\,,$$

$$(Z_1 - Z_2)\operatorname{Im}(Z_6^* Z_7) + \operatorname{Im}\big(Z_5^* Z_{67}^2\big) = 0\,,$$

where $Z_{ij} \equiv Z_i + Z_j$. The Type I, II, X, and Y Yukawa couplings arise after imposing the $\mathbb{Z}_2$ charges listed in the table below.

	Φ_1	Φ_2	U_R	D_R	E_R	$U_L,\ D_L,\ N_L,\ E_L$
Type I	$+$	$-$	$-$	$-$	$-$	$+$
Type II	$+$	$-$	$-$	$+$	$+$	$+$
Type X	$+$	$-$	$-$	$-$	$+$	$+$
Type Y	$+$	$-$	$-$	$+$	$-$	$+$

[†]See R. Boto, T.V. Fernandes, H.E. Haber, J.C. Romao, and J.P. Silva, Phys. Rev. D 101, 055023 (2020).

Type I: $\boldsymbol{\rho^F} = e^{i(\xi+\eta)}\sqrt{2}\boldsymbol{M_F}\cot\beta/v\,,$ where $F = U, D, E,$

Type II: $\boldsymbol{\rho^U} = e^{i(\xi+\eta)}\sqrt{2}\boldsymbol{M_U}\cot\beta/v\,,$ $\boldsymbol{\rho^{D,E}} = -e^{i(\xi+\eta)}\sqrt{2}\boldsymbol{M_{D,E}}\tan\beta/v\,,$

Type X: $\boldsymbol{\rho^{U,D}} = e^{i(\xi+\eta)}\sqrt{2}\boldsymbol{M_{U,D}}\cot\beta/v\,,$ $\boldsymbol{\rho^E} = -e^{i(\xi+\eta)}\sqrt{2}\boldsymbol{M_E}\tan\beta/v\,,$

Type Y: $\boldsymbol{\rho^{U,E}} = e^{i(\xi+\eta)}\sqrt{2}\boldsymbol{M_{U,E}}\cot\beta/v\,,$ $\boldsymbol{\rho^D} = -e^{i(\xi+\eta)}\sqrt{2}\boldsymbol{M_D}\tan\beta/v\,.$

The Type-I, II, X, and Y 2HDMs are special cases of the A2HDM, where the corresponding complex flavor-alignment parameters are:

1. Type-I: $a^U = a^D = a^E = e^{i(\xi+\eta)}\cot\beta.$

2. Type-II: $a^U = e^{i(\xi+\eta)}\cot\beta$ and $a^D = a^E = -e^{i(\xi+\eta)}\tan\beta.$

3. Type-X: $a^U = a^D = e^{i(\xi+\eta)}\cot\beta$ and $a^E = -e^{i(\xi+\eta)}\tan\beta.$

4. Type-Y: $a^U = a^E = e^{i(\xi+\eta)}\cot\beta$ and $a^D = -e^{i(\xi+\eta)}\tan\beta.$

The CP-conserving 2HDM

If the scalar potential and vacuum are CP-conserving, then there exists a *real Higgs basis* in which all Higgs basis scalar potential parameters are real. Thus, we set $s_{13} = 0$, $c_{13} = 1$ and $e^{i\eta} = \pm 1$. In particular, $e^{i\eta}$ changes sign under $\mathcal{H}_2 \to -\mathcal{H}_2$. One can identify[‡]

$$
\varepsilon \equiv e^{i\eta} = \begin{cases} \operatorname{sgn} Z_6 \,, & \text{if } Z_6 \neq 0, \\ \operatorname{sgn} Z_7 \,, & \text{if } Z_6 = 0 \text{ and } Z_7 \neq 0. \end{cases}
$$

[‡] If $Z_6 = Z_7 = 0$, then the sign of Z_5 is no longer invariant with respect to transformations that preserve the real Higgs basis (since the sign of Z_5 changes under $\mathcal{H}_2 \to \pm i\mathcal{H}_2$). In this case, it would be more appropriate to define $\varepsilon \equiv e^{2i\eta} = \operatorname{sgn} Z_5$.

To make contact with the standard notation of the CP-conserving 2HDM, under the assumption that the lighter of the two neutral CP-even Higgs bosons is SM-like, we make the following identifications:

$$h = h_1, \qquad H = -\varepsilon h_2, \qquad A = \varepsilon h_3, \qquad H^\pm \to \varepsilon H^\pm,$$

where the neutral CP-odd Higgs mass eigenstate is related to the Higgs basis fields by $A = \varepsilon \sqrt{2}\, \mathrm{Im}\, \mathcal{H}_2^0$ and

$$\begin{pmatrix} H \\ h \end{pmatrix} = \begin{pmatrix} c_{\beta-\alpha} & -s_{\beta-\alpha} \\ s_{\beta-\alpha} & c_{\beta-\alpha} \end{pmatrix} \begin{pmatrix} \sqrt{2}\, \mathrm{Re}\, \mathcal{H}_1^0 - v \\ \varepsilon\sqrt{2}\, \mathrm{Re}\, \mathcal{H}_2^0 \end{pmatrix},$$

where we have identified:

$$c_{12} = s_{\beta-\alpha}, \qquad\qquad s_{12} = -\varepsilon\, c_{\beta-\alpha}.$$

By convention, we choose $0 \leq \beta - \alpha \leq \pi$. Given the values of $\beta - \alpha$ and the masses of h, H, A and $H^{\pm}$, four of the seven real Higgs basis parameters Z_i are determined

$$Z_1 v^2 = m_h^2 s_{\beta-\alpha}^2 + m_H^2 c_{\beta-\alpha}^2 \,,$$

$$Z_4 v^2 = m_h^2 c_{\beta-\alpha}^2 + m_H^2 s_{\beta-\alpha}^2 + m_A^2 - 2m_{H^{\pm}}^2 \,,$$

$$Z_5 v^2 = m_h^2 c_{\beta-\alpha}^2 + m_H^2 s_{\beta-\alpha}^2 - m_A^2 \,,$$

$$|Z_6| v^2 = (m_H^2 - m_h^2) s_{\beta-\alpha} |c_{\beta-\alpha}| \,,$$

where $\varepsilon c_{\beta-\alpha} = -|c_{\beta-\alpha}| \leq 0$.[§]

In the CP-conserving A2HDM, the flavor alignment parameters are real.

[§]Note that both ε and $c_{\beta-\alpha}$ change sign under $\mathcal{H}_2 \to -\mathcal{H}_2$, whereas $\varepsilon c_{\beta-\alpha}$ is invariant.

The Yukawa Lagrangian is given by:

$$-\mathscr{L}_Y = \frac{1}{v} \sum_{F=U,D,E} \overline{F} M_{\boldsymbol{F}} \big[s_{\beta-\alpha} - a^F |c_{\beta-\alpha}| \big] F h$$

$$-\frac{1}{v} \sum_{F=U,D,E} \varepsilon \overline{F} M_{\boldsymbol{F}} \big[|c_{\beta-\alpha}| + a^F s_{\beta-\alpha} \big] F H$$

$$-\frac{i}{v} \sum_{F=U,D,E} \varepsilon_F \, \varepsilon \, a^F \, \overline{F} M_{\boldsymbol{F}} \gamma_5 F A$$

$$+\frac{\sqrt{2}}{v} \varepsilon \left\{ \overline{U} \big[a^D \boldsymbol{K} M_{\boldsymbol{D}} P_R - a^U M_{\boldsymbol{U}} \boldsymbol{K} P_L \big] D H^+ + a^E \overline{N} M_{\boldsymbol{E}} P_R E H^+ + \text{h.c.} \right\}$$

where we have introduced the notation,

$$\varepsilon_F = \begin{cases} +1 & \text{for } F = U \,, \\ -1 & \text{for } F = D, E \,. \end{cases}$$

The CP-conserving Type-I, II, X and Y 2HDMs are special cases of the A2HDM:

Type-I: $\quad a^U = a^D = a^E = \varepsilon \cot \beta$.

Type-II: $\quad a^U = \varepsilon \cot \beta$ and $a^D = a^E = -\varepsilon \tan \beta$.

Type-Y: $\quad a^U = a^E = \varepsilon \cot \beta$ and $a^D = -\varepsilon \tan \beta$.

Type-X: $\quad a^U = a^D = \varepsilon \cot \beta$ and $a^E = -\varepsilon \tan \beta$.

<u>REMARK</u>: In the 2HDM literature, the Φ-basis scalar fields are rephased such that $\xi = 0$ (i.e., the vevs are real and nonnegative), in which case $e^{i(\xi+\eta)} = \varepsilon$ and $\tan \beta \equiv \langle \Phi_2^0 \rangle / \langle \Phi_1^0 \rangle \geq 0$. Then $c_{\beta-\alpha}$ is promoted to a physical parameter and the sign of ε is fixed such that $\varepsilon c_{\beta-\alpha} \leq 0$.

To implement the CP-conserving Type-I, II, X and Y 2HDM, there must exist a real Φ-basis such that $\lambda_6 = \lambda_7 = 0$. Such a basis exists if $T_{Z_2} = 0$, where

$$T_{Z_2} \equiv \left| (Z_1 - Z_2)[Z_1 Z_7 + Z_2 Z_6 - (Z_3 + Z_4 + Z_5)(Z_6 + Z_7)] \right.$$
$$\left. + 2(Z_6 + Z_7)^2 (Z_6 - Z_7) \right|.$$

Scanning the CP-conserving A2HDM parameter space

The following parameters govern the CP-conserving A2HDM parameter space:

$$m_h, m_H, m_A, m_{H^\pm}, |c_{\beta-\alpha}|, Z_2, Z_3, Z_7, a^U, a^D, a^E.$$

Note that $\tan\beta$ is meaningful only in the special cases of Types I, II, X, and Y.

Parameter Intervals Scanned

|	
$\lvert c_{\beta-\alpha} \rvert$	0 , 0.45
Z_2	0 , 4.5
Z_3	-2 , 12
Z_7	-10 , 10
$m_{H^\pm}$	200 , 1000 GeV
a^U	-1.5 , 1.5
a^D	-50 , 50
a^E	-50 , 50

Table 5: Parameter intervals scanned in the analysis of Scenarios 1 and 2.

Theoretical and Experimental Constraints:

1. The scalar potential is bounded from below

2. Tree-level unitarity and perturbativity

3. The lightest Higgs scalar is SM-like and its properties are consistent with the current Higgs signal strength data

4. Precision electroweak constraints on the oblique parameters S and T

5. Heavy flavor constraints (most significant are $b \rightarrow s\, \gamma$ and ΔM_{Bs})[+]

6. Searches for new elementary scalar states at the LHC

[+] We use NLO results provided by T. Enomoto and R. Watanabe, JHEP 05, 002 (2016). We compared our results to A. Penuelas and A. Pich, JHEP 12, 084 (2017).

NLO $b \rightarrow s + \gamma$ Constraints
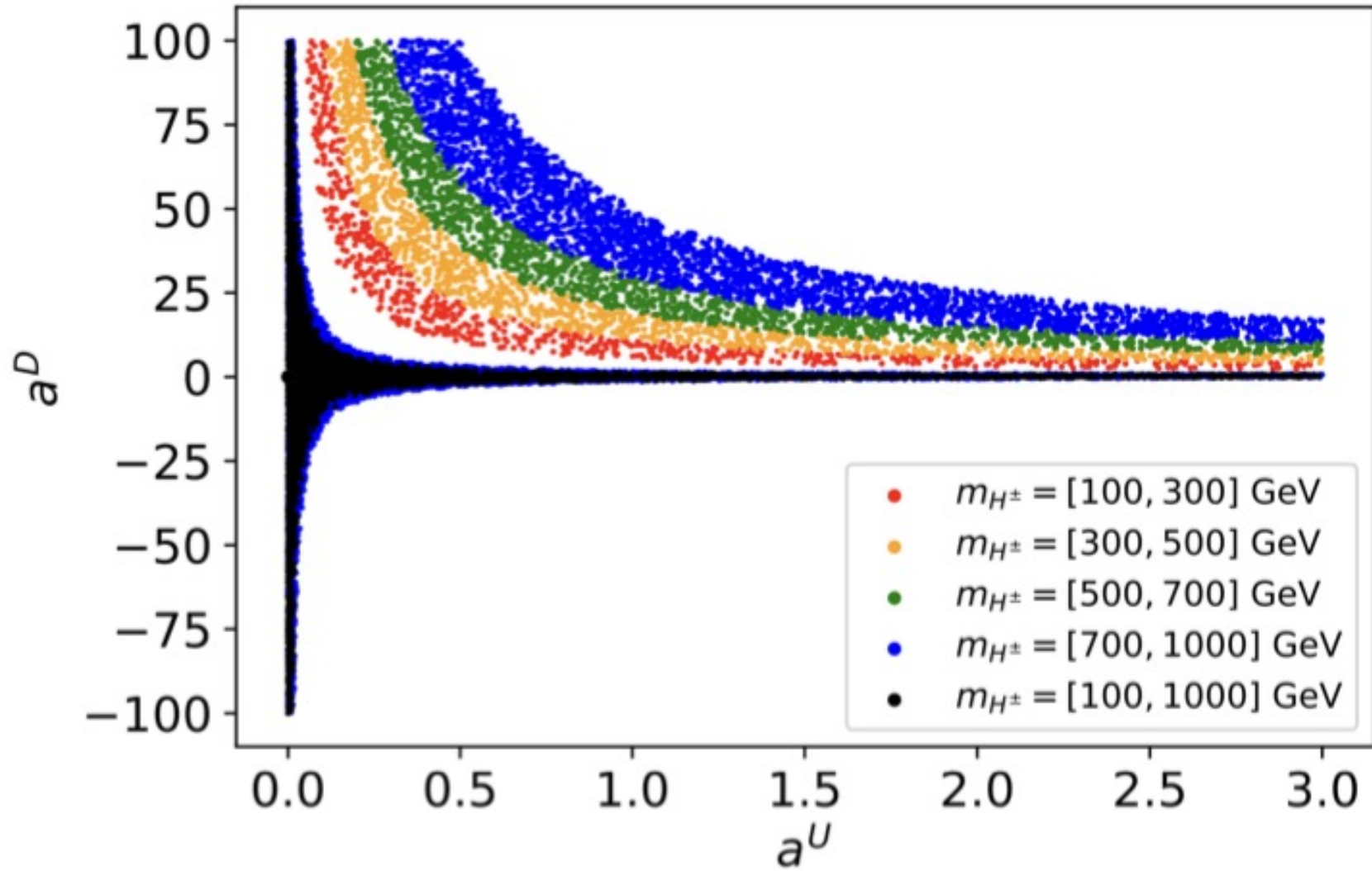
All points shown above satisfy $|\delta BR(b \rightarrow s\,\gamma)| \leq 4 \times 10^{-5}$.

Scenario 1: The A2HDM scan and implications for Types I, II, X and Y

Types II and Y ruled out due to b $\rightarrow$ s γ constraints. Dedicated Type I and Type X scans eliminate Type X but allow Type I.
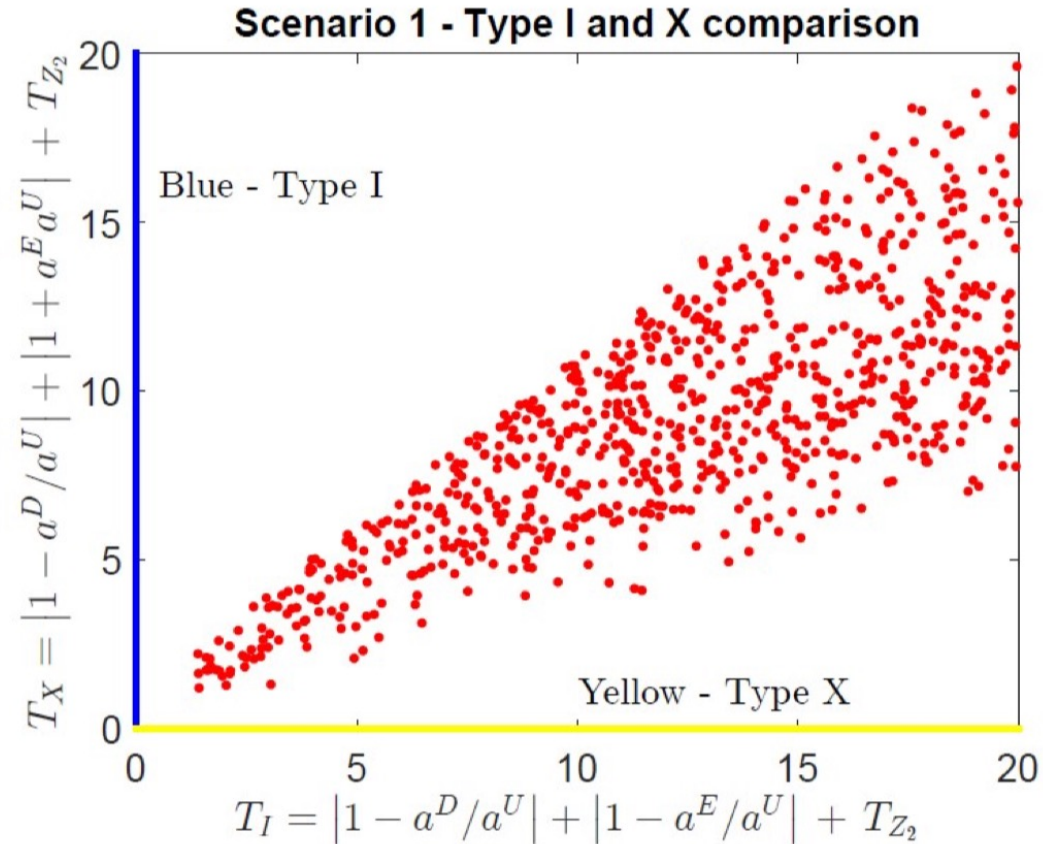

Figure 8: Results of a scan over A2HDM parameter points in Scenario 1 that satisfy the theoretical and experimental constraints elucidated in Section 4 and the constraints of eqs. (57)–(60) and eqs. (64)–(66). We plot the values of T_I vs. T_X for all surviving scan points. Points that lie along the horizontal (yellow) axis would be consistent with a Type-X 2HDM. Points that lie along the vertical (blue) axis would be consistent with a Type-I 2HDM.

Scenario 1: Type-I 2HDM benchmark point

Benchmark B1a – Type-I 2HDM				
$m_{H\pm}$ (GeV)	$\cos(\beta - \alpha)$	Z_2	Z_7	$\tan\beta$
650	-0.0013	2.27	0.58	4.0

Table 7: Parameters characterizing Benchmark B1a, for which $m_h = 125$, $m_A = 610$ and $m_H = 290$ GeV. The corresponding A2HDM flavor-alignment parameters satisfy $a^U = a^D = a^E = 1/\tan\beta \simeq 0.25$. Note that $\cos(\beta - \alpha) < 0$ in light of eqs. (33) and (41). The parameter $Z_3 = 11.89$ is obtained by imposing the condition for a softly-broken $\mathbb{Z}_2$ symmetric scalar potential by setting $T_{Z_2} = 0$ [cf. eq. (40)].

$\sigma(gg \to H)$ (pb)	0.65
$\sigma(gg \to b\bar{b}H)$ (pb)	1.9×10^{-3}
BR($H \to ZZ$)	0.0053
BR($H \to b\bar{b}$)	0.47
BR($H \to \tau^+\tau^-$)	0.053
BR($H \to hh$)	0.023
BR($H \to gg$)	0.41
Γ_H (GeV)	7×10^{-4}

$\sigma(gg \to A)$ (pb)	0.18
$\sigma(gg \to b\bar{b}A)$ (pb)	6.9×10^{-5}
BR($A \to ZH$)	0.94
BR($A \to t\bar{t}$)	0.057
BR($A \to b\bar{b}$)	1.9×10^{-5}
BR($A \to \tau^+\tau^-$)	2.0×10^{-6}
BR($A \to H^\pm W^\mp$)	0
Γ_A (GeV)	31.99

Table 8: Production cross sections and relevant decay branching ratios for H and A in benchmark B1a.

$\sigma(gg \to tbH^\pm)$ (pb)	0.0078
BR($H^\pm \to tb$)	0.040
BR($H^\pm \to \tau^\pm \nu$)	2.0×10^{-6}
BR($H^\pm \to HW^\pm$)	0.96
$\Gamma_{H^\pm}$ (GeV)	45.39

Table 9: Production cross sections and relevant decay branching ratios for $H^\pm$ in benchmark B1a.

Scenario 1: generic A2HDM benchmark point

Benchmark B1b – generic A2HDM							
$m_{H^\pm}$ (GeV)	$|\cos(\beta - \alpha)|$	Z_2	Z_3	Z_7	a^U	a^D	a^E
600	0.013	1.51	9.79	-0.20	0.20	1.75	3.50

Table 10: Parameters characterizing Benchmark B1b, for which $m_h = 125$, $m_A = 610$ and $m_H = 290$ GeV.

One can distinguish this benchmark point from Type-I by searching for gg → bbH → bbbb.

$\sigma(gg \to H)$ (pb)	0.40
$\sigma(gg \to b\bar{b}H)$ (pb)	0.096
BR$(H \to ZZ)$	0.015
BR$(H \to b\bar{b})$	0.61
BR$(H \to \tau^+\tau^-)$	0.28
BR$(H \to hh)$	0.053
Γ_H (GeV)	0.027

$\sigma(gg \to A)$ (pb)	0.11
$\sigma(gg \to b\bar{b}A)$ (pb)	0.0034
BR$(A \to ZH)$	0.96
BR$(A \to t\bar{t})$	0.036
BR$(A \to b\bar{b})$	9.47×10^{-4}
BR$(A \to \tau^+\tau^-)$	4.95×10^{-4}
Γ_A (GeV)	31.31

Table 11: Production cross sections and relevant decay branching ratios for H and A in benchmark B1b.

$\sigma(gg \to tbH^\pm)$ (pb)	0.0069
BR$(H^\pm \to tb)$	0.035
BR$(H^\pm \to \tau^\pm\nu)$	5.18×10^{-4}
BR$(H^\pm \to HW^\pm)$	0.96
$\Gamma_{H^\pm}$ (GeV)	29.38

Table 12: Production cross sections and relevant decay branching ratios for $H^\pm$ in benchmark B1b.
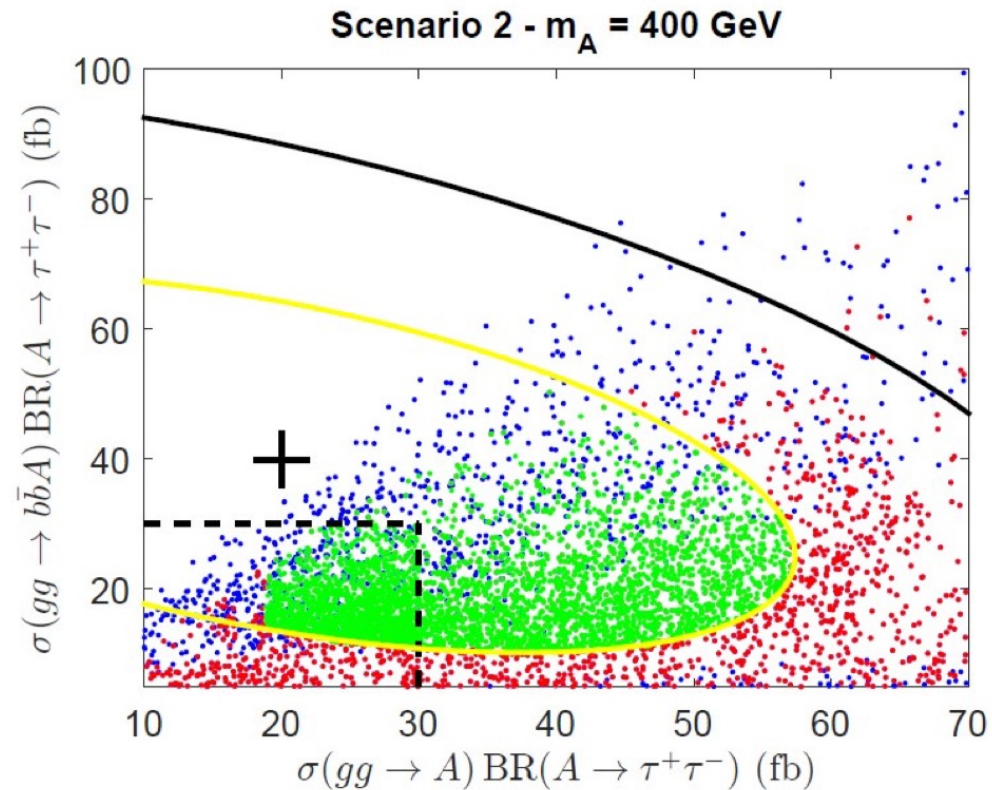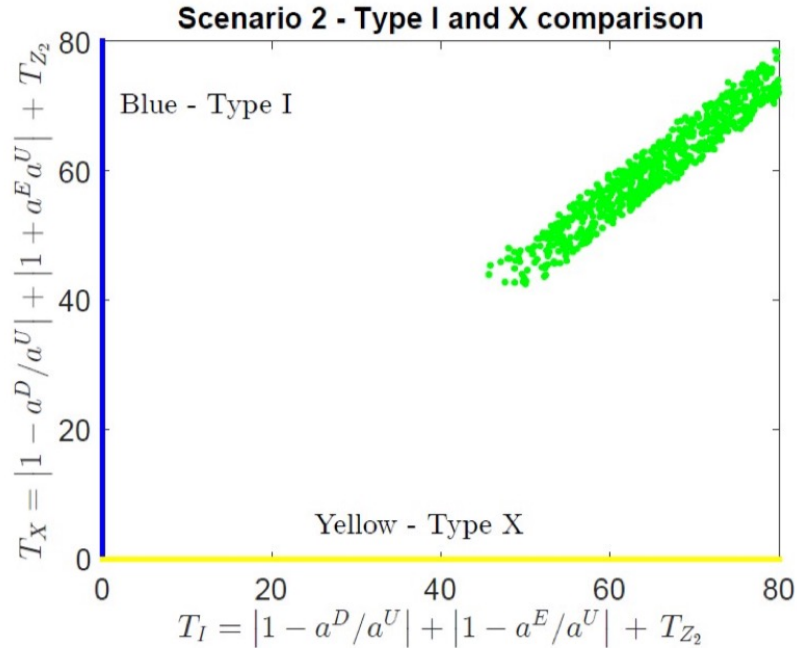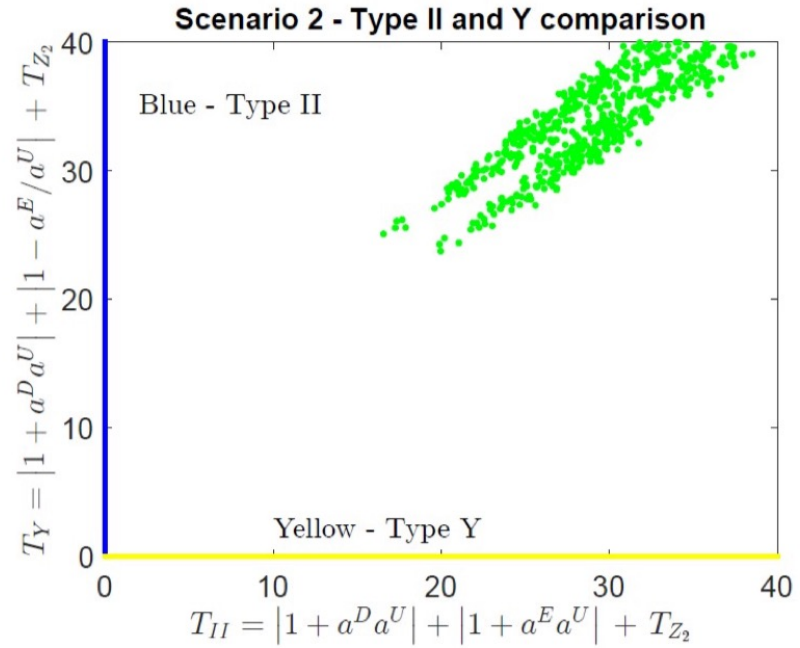
Scenario 2: A2HDM scan

Figure 10: Results of a scan over A2HDM parameter points in Scenario 2 that satisfy the theoretical and experimental constraints elucidated in Section 4. The blue points exhibit the values of the cross sections for gluon fusion production and b-associated production of A multiplied by $\mathrm{BR}(H \to \tau^+\tau^-)$. These points are colored red if the corresponding values of a^U and Γ/m_A lie in the red region of Fig. 9. The + indicates the best fit point for the ATLAS excess of Ref. [19] interpreted as A production with $m_A = 400$ GeV; the solid yellow and black curves correspond to the corresponding 1σ and 2σ contours. Red points within the 1σ contour are colored green. Finally, all points outside the dashed black boundary of the rectangular box are excluded at the 95% CL by the ditau search of the CMS Collaboration [22].

Among the viable A2HDM points, none of the Types I, II, X, and Y Yukawa coupling scenarios survive.

(a)

(b)

Figure 13: Results of a scan over A2HDM parameter points in Scenario 2 that lie within the region of interest, corresponding to the area of parameter space occupied by the subset of green points that lie inside the rectangular box in Fig. 10 and below the solid black lines in Fig. 11. Panel (a) exhibits the values of T_I vs. T_X. Points that lie along the horizontal (yellow) axis would be consistent with a Type-X 2HDM. Points that lie along the vertical (blue) axis would be consistent with a Type-I 2HDM. Panel (b) exhibits the values of T_{II} vs. T_Y. Points that lie along the horizontal (yellow) axis would be consistent with a Type-Y 2HDM. Points that lie along the vertical (blue) axis would be consistent with a Type-II 2HDM.

Scenario 2: generic A2HDM benchmark point

Benchmark B2 – generic A2HDM								
m_H	$m_{H^\pm}$ (GeV)	$|\cos(\beta-\alpha)|$	Z_2	Z_3	Z_7	a^U	a^D	a^E
492	529	0.0018	2.42	7.58	-1.39	0.60	35.07	6.32

Table 13: Parameters characterizing Benchmark B2, for which $m_h = 125$, $m_A = 400$ GeV.

$\sigma(gg \to H)$ (pb)	2.57
$\sigma(gg \to b\bar{b}H)$ (pb)	3.30
BR($H \to b\bar{b}$)	0.69
BR($H \to \tau^+\tau^-$)	0.0028
BR($H \to t\bar{t}$)	0.31
Γ_H (GeV)	14.54

$\sigma(gg \to A)$ (pb)	10.87
$\sigma(gg \to b\bar{b}A)$ (pb)	8.97
BR($A \to t\bar{t}$)	0.39
BR($A \to b\bar{b}$)	0.60
BR($A \to \tau^+\tau^-$)	0.0024
Γ_A (GeV)	13.94

Table 14: Production cross sections and relevant decay branching ratios for H and A in benchmark B2.

Promising channels for future LHC discoveries include bbH production followed by H → bb, tt.

$\sigma(gg \to tbH^\pm)$ (pb)	0.19
BR($H^\pm \to tb$)	0.90
BR($H^\pm \to \tau^\pm\nu$)	0.0023
BR($H^\pm \to AW^\pm$)	0.095
$\Gamma_{H^\pm}$ (GeV)	19.05

Table 15: Production cross sections and relevant decay branching ratios for $H^\pm$ in benchmark B2.

Parting messages

➤ If evidence for new heavy scalars emerges, the 2HDM provides a robust framework for interpretation.

➤ However, beware of over-constraining the 2HDM framework.

➤ Although Types I, II, X, and Y Yukawa couplings are theoretically favored, a more general set of (approximately) flavor-aligned Yukawa coupling can satisfy the experimental FCNC constraints.

➤ Ultimately, it is up to experimental observations to dictate the underlying structure of the Higgs-fermion Yukawa interactions.

➤ Scenario 2 provides an example of a case where the observations of a new heavy scalar is incompatible with Types I, II, X, and Y Yukawa couplings, but can be accommodated in a more generic A2HDM framework.
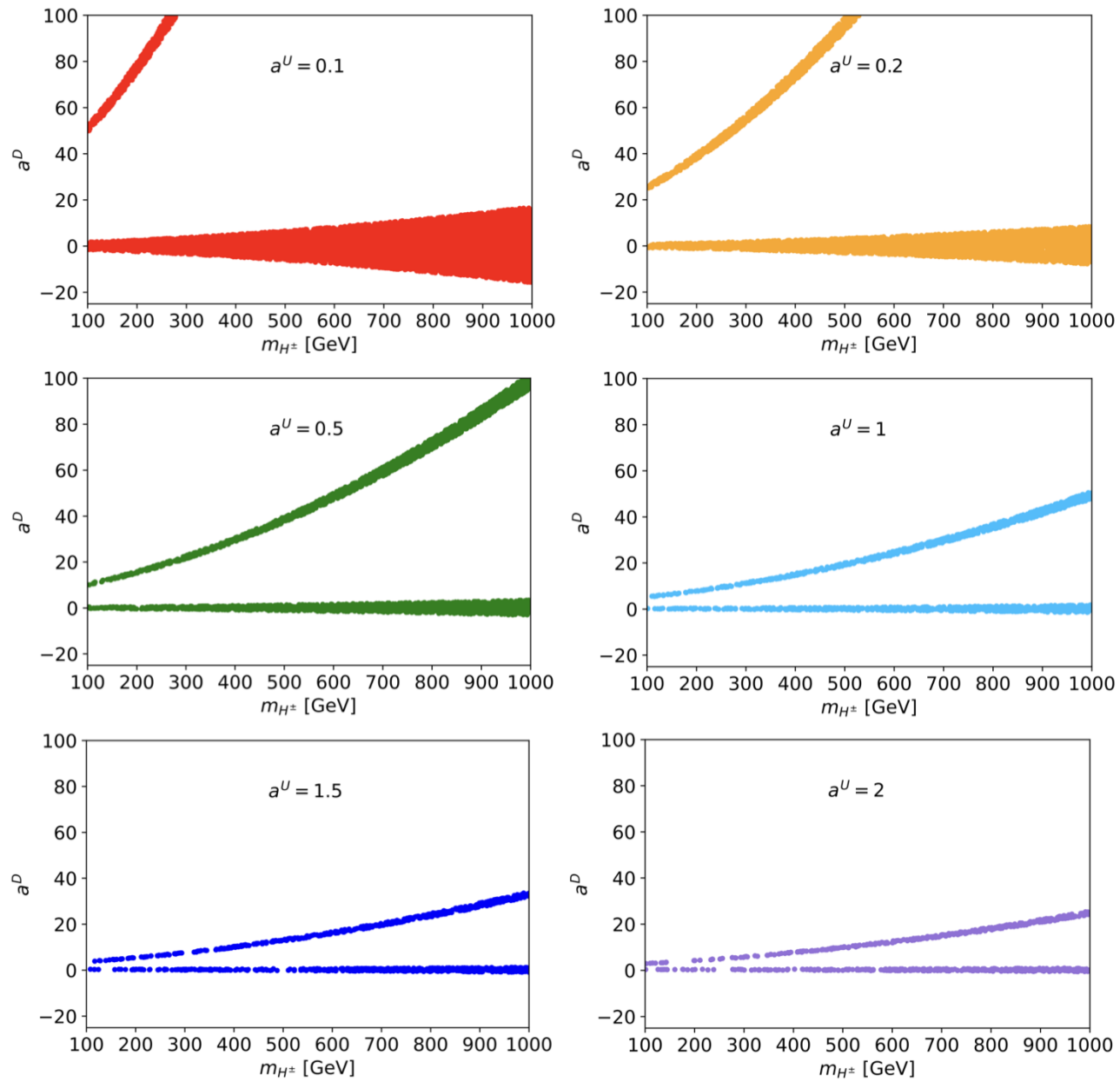
Backup slides

Figure 16: Regions of the A2HDM parameter space (indicated by the various colors) that satisfy $|\delta\mathrm{BR}(b \to s\gamma)| \leq 4 \times 10^{-5}$ for fixed values of $a^U = 0.1$, 0.2, 0.5, 1.0, 1.5 and 2.0. Combining the six panels above yields the plot shown in Fig. 15.

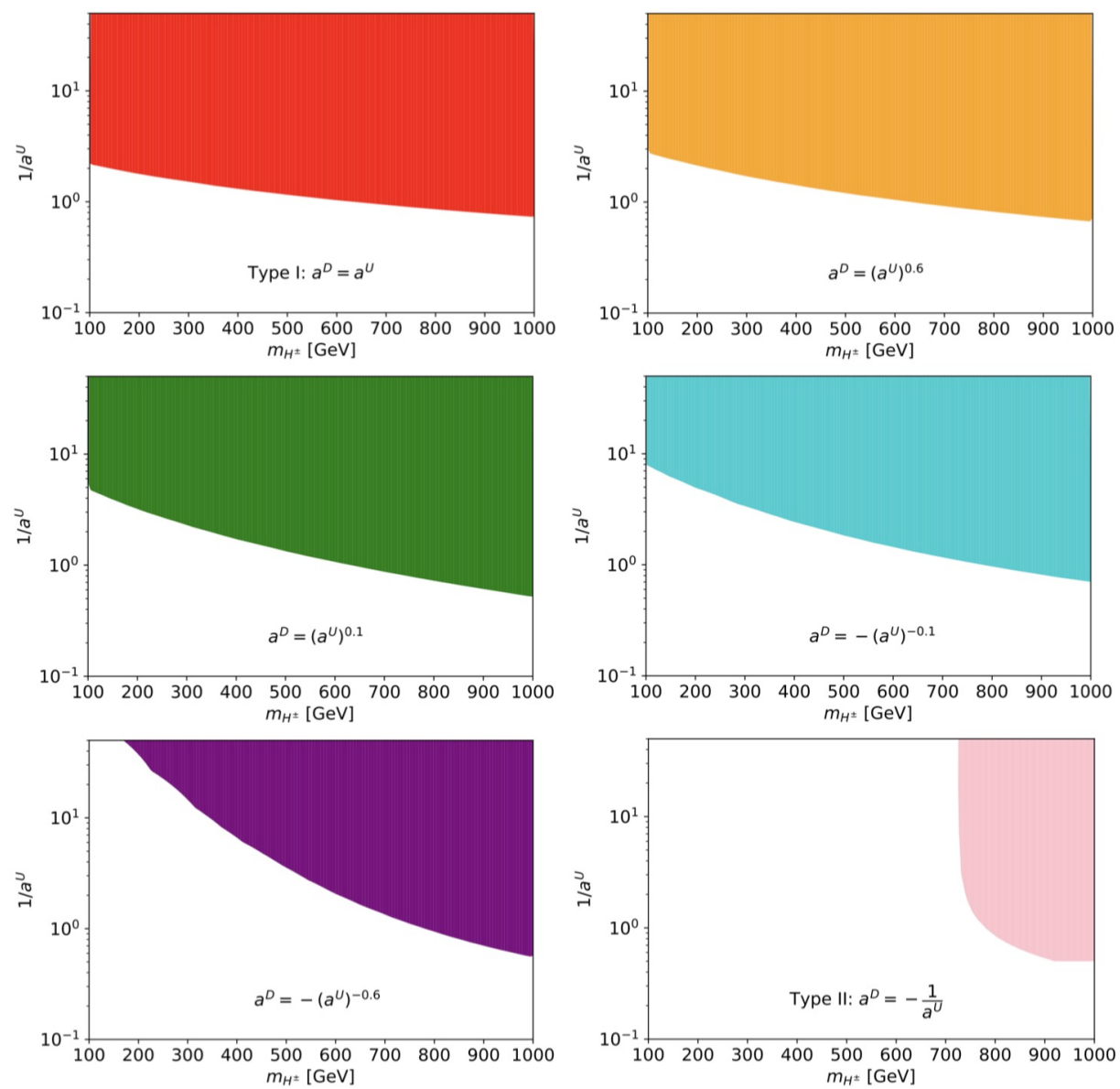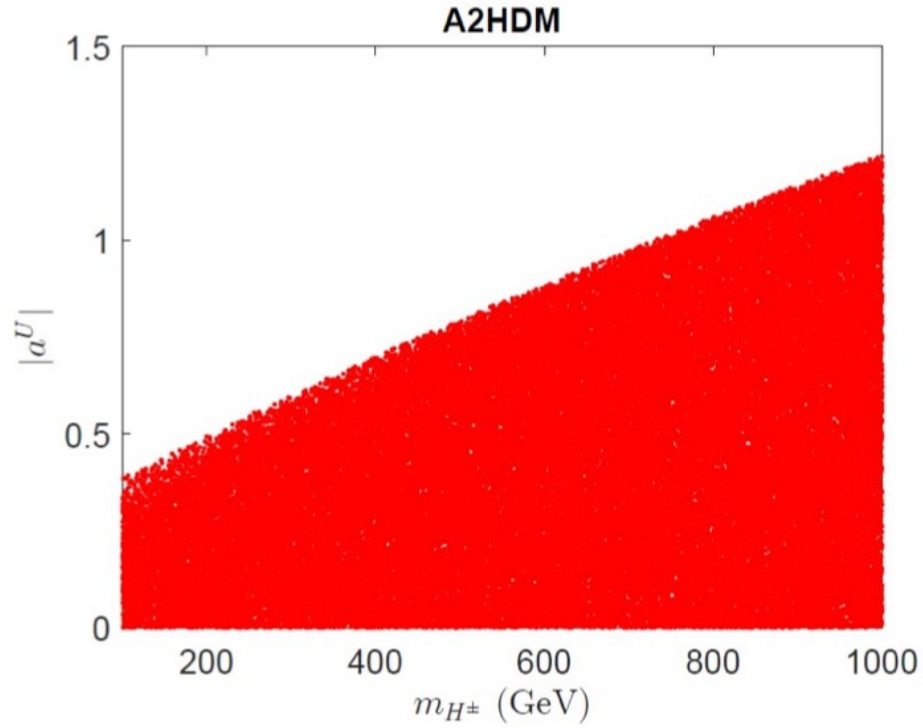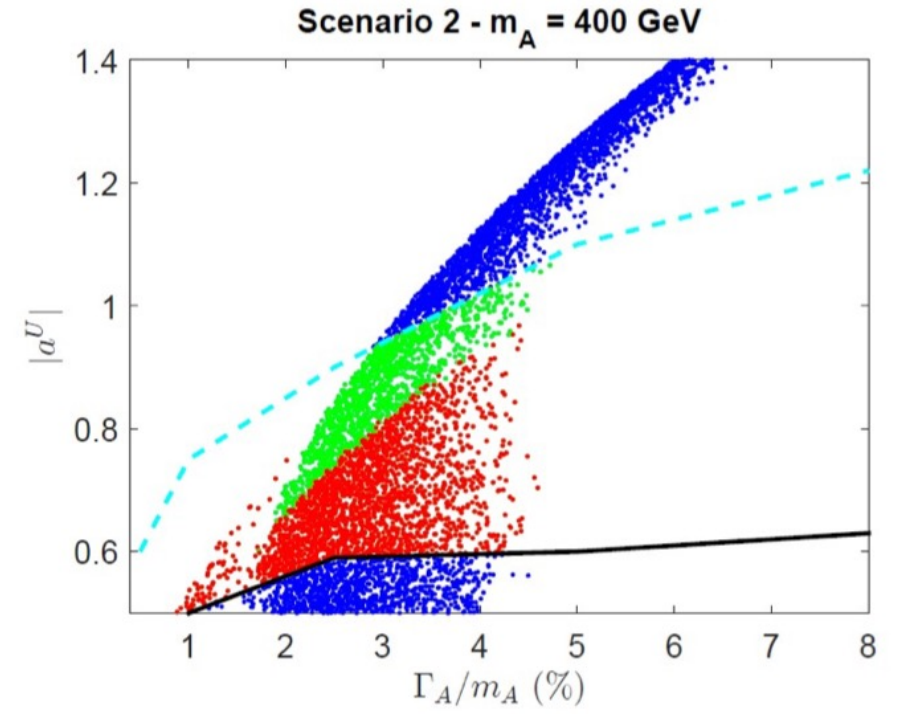Figure 17: Regions of the A2HDM parameter space (indicated by the various colors) in the $m_{H^\pm}$ vs. $1/a^U$ plane that satisfy $|\delta\mathrm{BR}(b \to s\gamma)| \leq 4 \times 10^{-5}$. The uncolored regions are excluded. The value of a^D is fixed by $a^D = (a^U)^p \, \mathrm{sgn}\, p$. As p varies, we include all parameter points in which $|a^D| < 100$. The sequence of panels correspond to $p = 1, 0.6, 0.1, -0.1, -0.6,$ and -1. The case of $p = 1$ [$p = -1$] corresponds to the Type I [Type II] 2HDM. In these two cases, in a convention where $\tan\beta$ is positive, one may identify $\tan\beta = 1/a^U$.

Figure 19: Impact of the ΔM_{B_s} bound on the A2HDM parameter space. In panel (a) all points shown are from a general scan on a^U, a^D and $m_{H^\pm}$ which pass the ΔM_{B_s} bound. In panel (b) we exhibit the ratio of the A width to its mass (with $m_A = 400$ GeV) as a function of the flavor-alignment parameter $|a^U|$ in Scenario 2. The blue points are the result of a scan over A2HDM parameters, subject to the theoretical and experimental constraints elucidated in Section 4 prior to imposing the ΔM_{B_s} bound. The dashed cyan (solid black) line correspond to the observed (expected) 95% CL upper limit on the cross section for $gg \to A \to t\bar{t}$ reported by the CMS Collaboration in Ref. [21], translated into an upper limit for $|a^U|$ as a function of Γ_A/m_A. As for the remaining scan points that lie between the dashed cyan and solid black curve, the green points are eliminated after imposing the ΔM_{B_s} constraint. The surviving red scan points constitute the proposed signal of Scenario 2.

Origin of the $e^{i(\xi+\eta)}$ factor

The alignment parameters a^F are basis-invariant quantities, which have been written above in terms of the Φ-basis parameters. Consider a new Φ'-basis that is related to the Φ-basis via $\Phi' = U\Phi$, where

$$U = \begin{pmatrix} 0 & e^{-i\xi} \\ e^{i\zeta} & 0 \end{pmatrix}.$$

In the Φ'-basis, the roles of Φ_1 and Φ_2 are interchanged with respect to the Φ-basis. Thus, the softly broken $\mathbb{Z}_2$ symmetry is also manifestly realized in the Φ'-basis, where the $\mathbb{Z}_2$ charges of Φ_1 and Φ_2 specified in table of $\mathbb{Z}_2$ charges are interchanged.

We shall refer to the corresponding Yukawa couplings in the Φ'-basis as Type I$'$, Type II$'$, etc. In particular, in light of

$$\begin{pmatrix} s_\beta \\ c_\beta e^{i\zeta} \end{pmatrix} = U \begin{pmatrix} c_\beta \\ s_\beta e^{i\xi} \end{pmatrix},$$

we conclude that $\beta' = \frac{1}{2}\pi - \beta$ and $\xi' = \zeta$. Moreover, in light of $e^{i\eta'} = (\det\ U)^{-1}e^{i\eta}$ and $\det U = -e^{i(\zeta - \xi)}$, it follows that

$$e^{i(\xi' + \eta')} = -e^{i(\xi + \eta)}.$$

Thus, with respect to the parameters of the Φ'-basis, the expressions for a^F are modified by interchanging $\tan\beta \leftrightarrow \cot\beta$ and multiplying the resulting expressions by -1. But these are precisely the results for a^F that would have been obtained by employing the Type-I$'$ and Type-II$'$ Yukawa couplings.